The *N. gonorrhoeae* Type IV Pilus Stimulates Mechanosensitive Pathways and Cytoprotection through a *pilT*-Dependent Mechanism

Heather L. Howie[1*], Michael Glogauer[2], Magdalene So[1]

1 Department of Molecular Microbiology and Immunology, Oregon Health and Science University, Portland, Oregon, United States of America, **2** Canadian Institutes of Health Research Group in Matrix Dynamics, University of Toronto, Ontario, Canada

The *Neisseria gonorrhoeae* type IV pilus is a retractile appendage that can generate forces near 100 pN. We tested the hypothesis that type IV pilus retraction influences epithelial cell gene expression by exerting tension on the host membrane. Wild-type and retraction-defective bacteria altered the expression of an identical set of epithelial cell genes during attachment. Interestingly, pilus retraction, per se, did not regulate novel gene expression but, rather, enhanced the expression of a subset of the infection-regulated genes. This is accomplished through mitogen-activated protein kinase activation and at least one other undefined stress-activated pathway. These results can be reproduced by applying artificial force on the epithelial membrane, using a magnet and magnetic beads. Importantly, this retraction-mediated signaling increases the ability of the cell to withstand apoptotic signals triggered by infection. We conclude that pilus retraction stimulates mechanosensitive pathways that enhance the expression of stress-responsive genes and activate cytoprotective signaling. A model for the role of pilus retraction in influencing host cell survival is presented.

Citation: Howie HL, Glogauer M, So M (2005) The *N. gonorrhoeae* type IV pilus stimulates mechanosensitive pathways and cytoprotection through a *pilT*-dependent mechanism. PLoS Biol 3(4): e100.

Introduction

Many pathogenic and nonpathogenic bacteria produce type IV pili (Tfp), among them, *Neisseria gonorrhoeae*, *N. meningitidis*, *Pseudomonas aeruginosa*, *Legionella pneumophila*, enteropathogenic and enterohemorrhagic *Escherichia coli*, and *Vibrio cholerae* [1]. Tfp are fimbriate organelles that play a crucial role in the interaction of the bacterium with its environment, as evidenced by their requirement for motility [2], biofilm formation [3,4], and horizontal gene transfer [5,6,7]. These appendages also promote bacterial attachment to host cells and contribute to virulence [8,9,10,11,12].

Recent evidence has shown that the gonococcal Tfp can physically retract—a process that underlies twitching motility [13] (i.e., the ability of the bacterium to move on solid surfaces [14]). It is now generally believed that twitching motility occurs via extension, substrate tethering, and retraction of the pilus filament. Two inner membrane/cytoplasmic ATPases, PilF and PilT, take part in these activities. PilF mediates pilus assembly, as *pilF* mutants produce pilin subunits but are not piliated [15]. PilT is involved in pilus disassembly, as *pilT* mutants are piliated but cannot retract their pili [13,16]. Neither mutant is motile.

Pilus retraction allows gonococci to form organized microbial communities on the cell surface and on synthetic substrates (S. Lee and M. S., unpublished data), via both specific and nonspecific interactions. During attachment to host cells, microcolonies stimulate the formation of cortical plaques—structures in the cell cortex containing high concentrations of transmembrane receptors, nonreceptor tyrosine kinases and their anchors, and components of the cortical cytoskeleton [10,17]. Though *pilT* mutants adhere normally to both synthetic surfaces and epithelial cells, they form disordered microcolonies, fail to induce cortical plaques, and are less invasive than their wild-type (wt) parent strain [17].

Retraction of a single gonococcal pilus can exert forces up to 80–100 pN on its substrate [13,18]. Forces of lesser magnitude can elongate the membrane into microvillus-like structures [19,20], promote cytoskeleton rearrangements and protein clustering [21,22], induce calcium fluxes [23,24], and alter gene expression [25,26,27,28]. Pilus retraction has therefore been speculated to induce host cell signaling by exerting mechanical tension on the membrane [17]. Indirect support for a mechanical signaling hypothesis comes from observations that *pilT* mutants, unlike wt piliated strains, can neither trigger cortical plaque formation [10] nor activate PI-3 kinase (S. Lee and M. S., unpublished data), a member of a mechanical stress–activated pathway. Moreover, a *pilT* mutant induces an attenuated calcium flux in epithelial cells, as compared to infection with wt gonococci (P. Ayala and M. S., unpublished data). Here we provide further evidence that pilus retraction acts as a mechanical stimulus by activating

Received July 19, 2004; Accepted January 18, 2005; Published March 22, 2005
DOI: 10.1371/journal.pbio.0030100

Abbreviations: BSA, bovine serum albumin; CPP, crude pili preparation; MAPK, mitogen-activated protein kinase; PARP, poly(ADP-ribose) polymerase; STS, staurosporine; Tfp, type IV pili; W/P, wild-type to *pilT* fold-change expression ratio; wt, wild-type

Academic Editor: Matt Waldor, Tufts University School of Medicine, United States of America

*To whom correspondence should be addressed. E-mail: howieh@ohsu.edu

mechanical stress–signaling pathways that alter epithelial cell gene expression and generate a cytoprotective environment within the host cell.

Results

Pilus Retraction Enhances the Expression of Cell Stress/Survival Genes

We used microarrays to examine the transcriptional profiles of T84 human colorectal epithelial cells infected with retraction-proficient (N400) or retraction-deficient (N400*pilT*) gonococci for 3 h. Infection with N400 or N400*pilT* induced transcriptional changes in the same genes. Contrary to expectations, no genes responded uniquely to infection with either strain. Instead, infection with *pilT* affected the level of expression of a small subset of infection-responsive genes. To segregate the genes responding to pilus retraction, a wt to *pilT* fold-change expression ratio (W/P) was calculated for each infection-regulated gene. This method identified, out of approximately 300 infection-regulated genes, 69 probe sets (representing 52 genes) whose expression appeared to be enhanced by pilus retraction (Figure 1).

To confirm the microarray results, real-time quantitative RT-PCR was initially performed on two infection-regulated genes, *DUSP5* and *ADM*. According to our microarray data, *DUSP5* expression was enhanced by pilus retraction (W/P = 1.63), and *ADM* expression was not (W/P ≈ 1.0). RT-PCR results corroborated the microarray analysis, as *DUSP5* transcript levels were significantly higher in N400-infected cells than N400*pilT*-infected cells, whereas *ADM* transcript levels were similar in both sets of cells (Figure 2A). Ten additional genes predicted to respond to retraction and five additional genes predicted to be not affected by retraction were similarly analyzed by real-time quantitative RT-PCR (Figure 2B). In every case, the presumptive positives yielded W/P ratios of 1.5 or more, whereas the presumptive negatives yielded W/P ratios of approximately 1.0.

The identification of genes whose expression is enhanced by pilus retraction raised the question of whether these genes share a common regulatory pathway or perform similar functions. The majority of genes whose expression is enhanced by retraction are involved in the cell stress response and survival (Figure 2C). Over half of these can be induced by environmental or other cellular stresses, and a striking number can be induced specifically by mechanical stress (Figure 2D). Importantly, the majority of the genes from both groups can also be induced by mitogen-activated protein kinases (MAPKs; Figure 2D) (For literature citations, see Table S1.) These results indicate that pilus retraction may enhance infection-induced gene expression through the MAPK pathway.

ERK, JNK, and P38 MAPK Are Activated by Infection and Enhanced by Pilus Retraction

The MAPK cascades are well known for their involvement in the stress response, including the response to bacterial

Gene	Affy ID	GenBank	WT	*pilT*	W/P	p value
NR4A1	279_at	L13740	26.93	12.25	2.23	2.10E-06
NR4A1	280_g_at	L13740	23.43	13.10	1.81	2.03E-05
FOS	2094_s_at	K00650	22.53	11.80	1.88	5.09E-04
IL-8	1369_s_at	M28130	19.88	12.55	1.59	1.08E-05
DUSP1	1005_at	X68277	19.74	6.50	3.04	2.06E-06
IL-8	35372_r_at	M17017	19.16	12.75	1.52	1.59E-02
IL-6	38299_at	X04430	18.56	8.29	2.45	3.05E-07
DUSP5	529_at	U15932	16.58	10.25	1.63	7.28E-07
NR4A2	547_s_at	S77154	15.10	8.00	1.89	2.33E-02
EGR2	37863_at	J04076	13.32	8.60	1.63	3.65E-01
DTR	38037_at	M60278	12.77	7.63	1.69	4.16E-02
GRO1	408_at	X54489	9.39	5.78	1.63	1.74E-04
GRO2	37187_at	M36820	9.01	5.60	1.71	1.35E-05
TNFalpha	1852_at	X02910	8.33	3.32	2.56	3.94E-04
SOCS3	40968_at	AB004904	8.29	5.49	1.53	2.23E-01
JUNB	2049_s_at	M29039	8.29	5.66	1.46	1.62E-03
Id1	36619_r_at	S78825	8.18	4.98	1.63	1.08E-02
TCF8	33439_at	D15050	7.77	5.10	1.53	6.39E-03
GRO3	34022_at	M36821	7.73	5.18	1.53	9.01E-04
H2BFR	35562_at	AI076718	7.17	3.27	4.16	2.78E-02
H2AF0	32609_at	AI885852	6.64	2.63	2.55	3.07E-03
BLIMP1	31779_s_at	AF084199	6.15	4.25	1.59	9.40E-02
ATF3	287_at	L19871	5.88	3.47	1.68	1.06E-03
KRT16	601_s_at	M28439	5.44	2.61	1.89	2.07E-03
CSF2	1400_at	M13207	5.12	2.97	1.69	2.93E-03
NR4A2	37623_at	X75918	5.03	2.93	1.73	8.57E-02
CYR61	38772_at	Y11307	4.98	2.35	2.15	6.92E-07
H2AF0	286_at	L19779	4.79	2.17	2.22	1.10E-03
CSF2	1401_g_at	M13207	4.57	2.52	1.80	2.99E-03
DUSP2	1292_at	L11329	4.51	3.07	1.53	1.96E-03
EGR1	789_at	X52541	4.46	2.57	1.74	2.22E-03
H2AFA	35127_at	AI039144	4.38	1.86	2.38	2.40E-02
OVOL1	34047_at	AF016045	4.20	2.30	1.81	1.08E-03
uPA	37310_at	X02419	4.09	2.65	1.53	3.01E-03
GADD45B	39822_s_at	AF078077	3.89	1.96	2.01	3.97E-02
GADD34	37028_at	U83981	3.66	2.56	1.47	6.29E-03
RHOB	1826_at	M12174	3.10	1.94	1.58	8.58E-03
	37538_at	AL049354	3.08	1.28	2.17	6.16E-02
HSP70-2	31692_at	M59830	3.00	1.59	2.02	1.92E-01
H1F2	37018_at	AI189287	2.86	1.81	1.64	6.68E-01
Id1	36618_g_at	X77956	2.83	1.81	1.58	1.17E-03
KIP2	38673_s_at	D64137	2.52	1.55	1.62	3.07E-03
HBP17	38489_at	M60047	2.47	1.71	1.48	2.32E-04
RHO6	37785_at	U69563	2.46	1.70	1.47	1.08E-03
MIP1A	36103_at	D90144	2.38	1.52	1.57	3.60E-03
HSPF1	752_s_at	D85429	2.32	1.54	1.59	1.24E-02
MEKK1	33009_at	AF042838	2.18	0.95	2.30	3.13E-02
KIP2	1787_at	U22398	2.04	1.30	1.57	4.31E-02
H3FB	34964_at	N35832	2.01	1.35	1.53	1.21E-01
	38207_at	AW006742	1.94	1.32	1.47	1.14E-01
E2F-2	37043_at	AL021154	1.63	1.04	1.57	5.06E-04
CYP1A1	1024_at	X02612	-1.75	-1.12	1.57	3.36E-02
FDZF2	38872_at	U95044	-1.94	-1.19	1.63	2.29E-01
	36070_at	AL049389	-1.94	-1.23	1.57	4.56E-03
ZNF253	35573_r_at	AF038951	-1.94	-1.23	1.57	2.28E-02
PLXNC1	32193_at	AF030339	-1.99	-1.24	1.59	4.50E-01
ALDH1A3	36686_at	U07919	-2.00	-1.28	1.57	1.09E-03
CYP1A1	1025_g_at	X02612	-2.01	-1.28	1.57	1.39E-02
CYP1A1	36767_at	K03191	-2.04	-1.35	1.52	1.60E-02
	40143_at	D50930	-2.23	-1.52	1.47	8.01E-03
SOCS5	32669_at	AB014571	-2.23	-1.24	1.80	5.29E-02
	34283_at	AL050125	-2.57	-1.32	1.94	1.05E-01
	40848_g_at	AB018293	-2.75	-1.81	1.52	5.37E-02
CBX6	39560_at	H10776	-2.86	-1.99	1.47	5.07E-01
SIM2	39608_at	U80456	-2.95	-1.87	1.57	1.05E-01
	41807_at	AL040137	-3.04	-1.94	1.57	3.61E-02
EIF2C2	38505_at	AL050151	-3.19	-2.04	1.57	1.82E-02
GRLF1	34724_at	AI670100	-3.64	-1.63	2.18	9.81E-02
ZNF211	38142_at	U38904	-4.71	-1.63	2.81	5.06E-02

Fold Change
>6.0
3.0 to 5.9
1.0 to 2.9
-1.0 to -1.9
-2.0 to -2.9
<-3.0

W/P Ratio
1.5 to 1.9
2.0 to 2.4
>2.5

p value
>.05
.05 to .01
.01 to .001
<.001

Figure 1. Infection-Regulated, Retraction-Enhanced Epithelial Cell Genes

Wt and *pilT* values represent the mean fold-change in the transcript level of each gene in infected cells compared to uninfected cells ($n = 2$). W/P values represent the degree of enhancement of gene expression resulting from pilus retraction and are the result of dividing the wt fold-change value by the *pilT* fold-change value from two independent experiments. The *p*-value for each gene represents the statistical significance of the difference in its expression level (as determined by Cyber-T analysis) between wt and *pilT*. The color code assigned to each gene represents its degree of response to infection as expressed by its fold-change value, W/P, and *p*-value.

DOI: 10.1371/journal.pbio.0030100.g001

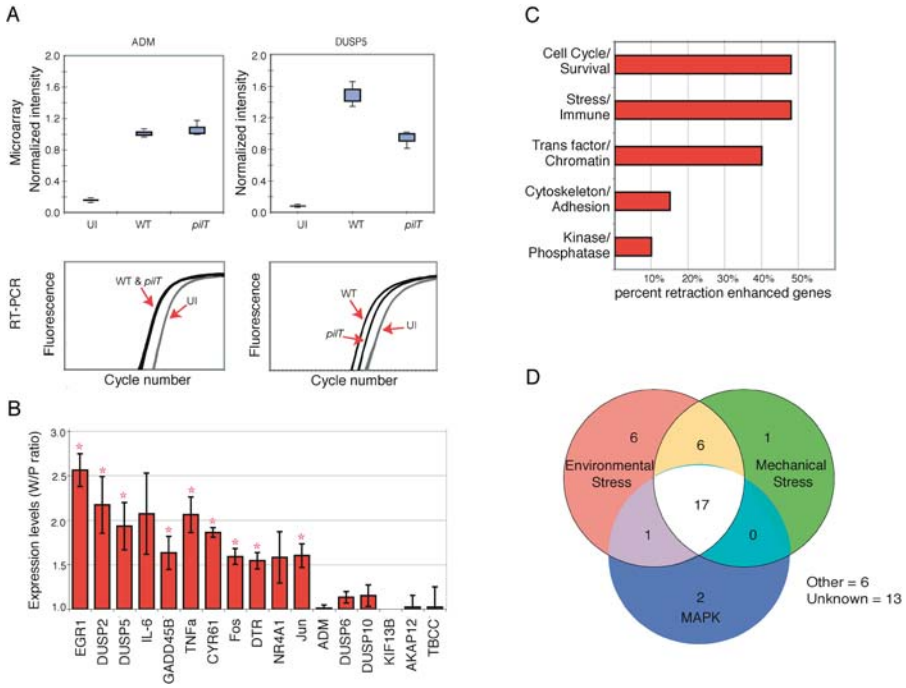

Figure 2. Real-Time Quantitative RT-PCR Verification of Microarray Results and Initial Characterization of Retraction-Enhanced Genes

(A) Microarray (top panels) and real-time quantitative RT-PCR (bottom panels) expression profiles of ADM and DUSP5 in uninfected cells (UI), N400-infected cells (WT), and N400*pilT*-infected cells *(pilT)*. Microarray data are shown as box-plots ($n = 3$). RT-PCR data are plotted as triplicate samples from one representative experiment.

(B) Real-time quantitative RT-PCR verification of retraction-enhanced expression of selected genes. Data are expressed as average W/P (±SEM, $n = 3$). Genes with a W/P statistically greater than 1.0 ($p < 0.05$) are denoted with an asterisk.

(C) Grouping of retraction-enhanced genes according to function, based on published reports (see Table S1). Some genes have multiple functions and thus appear in more than one group.

(D) Genes in this study that are known to be induced by environmental stress, mechanical stress, or MAPK signaling (see Table S1).

DOI: 10.1371/journal.pbio.0030100.g002

infection. Previous studies have shown that JNK is activated in *N. gonorrhoeae*–infected HeLa, Chang, and phagocytic cells [29,30], and MAPK signaling is induced in conjunctival cells by *N. meningitidis* (R. Bonnah and M. S., unpublished data). To study the role of MAPK signaling in retraction-enhanced gene expression, we first determined which of these pathways are activated in infected T84 cells.

Compared to resting cells (Figure 3A, left panel), the addition of medium alone slightly increased the levels of ERK-p, JNK-p, and P38-p (Figure 3A, UI), but levels of each phosphorylated kinase returned to baseline after 90 min. Infection with N400 dramatically increased the levels of all three activated kinases by 60 min post-infection (Figure 3A, WT). Densitometric analysis of immunoblots from two independent experiments is shown in Figure 3B. ERK-p levels were elevated throughout the course of infection, with only a slight decrease in phosphorylation visible by 3 h post-infection. In contrast, P38-p and JNK-p levels peaked between 60 and 90 min post-infection and dropped noticeably by 3 h post-infection.

We next examined MAPK phosphorylation in T84 cells infected with N400*pilT* to determine whether kinase activation was influenced by pilus retraction. Low levels of all three activated MAPKs were detected in N400*pilT*-infected cells only after 90 min of infection (Figure 3A, PT). Densitometric analysis of immunoblots from two independent experiments is shown in Figure 3C. Although the kinetics of MAPK activation appear to be different in wt- and *pilT*-infected cells, a firm conclusion cannot be drawn from these results, given the delayed onset of activation and the low levels of phosphorylation of each enzyme. Taken together, these results demonstrate that infection by piliated gonococci activates all three MAPK pathways and that pilus retraction enhances this activation.

MAPK Signaling Is a Mediator of Retraction-Dependent Enhancement of Gene Expression

We next determined whether MAPK signaling regulates the expression of retraction-enhanced genes. T84 cells were preincubated with vehicle or MAPK inhibitors SB203588, U0126, and SP600125, and assessed for ERK, P38, and JNK activation by immunoblotting for ERK-p, MAPKAPK2-p, and c-Jun-p, respectively. MAPK inhibitors dramatically reduced the levels of all three activated kinases in both uninfected and N400-infected cells (Figure 3D). They also significantly reduced the transcript levels of four of the five retraction-responsive genes in N400-infected cells, as judged by real-time quantitative RT-PCR (Figure 3E). In contrast, the inhibitors did not affect the transcript levels of genes with a W/P of approximately 1.0. Interestingly, *cyr61* expression was unaltered by MAPK inhibitors. This gene was shown by microarray (W/P = 2.15) and RT-PCR analysis (W/P = 1.86) to respond to retraction. These results implicate MAPK signaling in the regulation of some, but not all, retraction-responsive genes. They indicate that other pathways also influence the response of genes to pilus retraction.

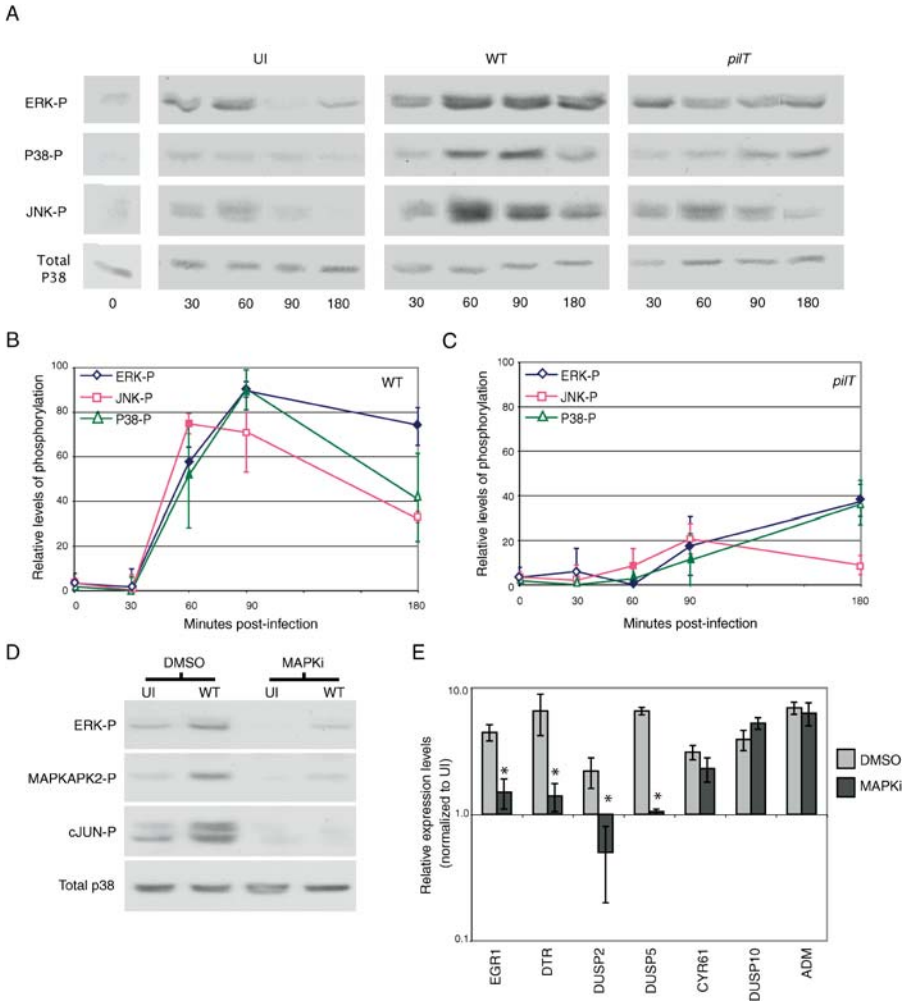

Figure 3. Levels of Activated MAPK in Infected Cells and Their Involvement in Retraction-Enhanced Gene Expression

(A) Representative immunoblot showing ERK-p, P38-p, and JNK-p, in uninfected cells before (0 h) and after medium change (UI), or in cells infected with N400 (WT) or N400*pilT (pilT)*. Total P38 protein levels in each sample served as the internal control (bottom lanes).
(B and C) ERK-p JNK-p, and P38-p levels over time in cells infected with N400 and N400*pilT*, respectively. Immunoblots from (A) were analyzed by densitometry, and levels of activated kinase from infected cells were normalized to that from uninfected cells (UI). Values represent mean normalized protein levels (±SEM, $n = 2$). Solid markers indicate a significant difference between wt and *pilT*-induced MAPK phosphorylation at that time point ($p < 0.05$); thus, ERK-p is significant at 60, 90, and 180 min; JNK-p is significant at 60 min; and P38-p is significant at 60 and 90 min.
(D) Representative immunoblot showing ERK-p, MAPKAPK2-p, and c-Jun-p in cells preincubated with vehicle (DMSO) or MAPK inhibitors and infected for 90 min with N400 (WT) or left untreated (UI). Total P38 protein levels in each sample served as the internal control (bottom lanes).
(E) Real-time quantitative RT-PCR analysis of the effect of MAPK inhibitors on the expression of retraction-responsive genes. Light bars indicate cells infected with N400 in the presence of vehicle (DMSO); dark bars indicate cells infected with N400 in the presence of MAPK inhibitors. Values represent the fold-change (±SEM, $n = 2$) in transcript levels compared to uninfected, DMSO treated control. A significant difference in expression between the two conditions is denoted by an asterisk ($p < 0.1$).
DOI: 10.1371/journal.pbio.0030100.g003

Mechanical Stress Activates MAPK Signaling and Upregulates Retraction-Responsive Genes

A significant number of the retraction-responsive genes are known to be induced specifically by mechanical strain on the cell membrane. Although substantial force is generated by pilus retraction in vitro, this force has not yet been demonstrated to influence host responses to infection. To examine this issue, we determined whether artificial mechanical force on the epithelial cell membrane could mimic retraction-induced MAPK activation and retraction-enhanced gene expression. To generate mechanical stress in a manner similar to that of pilus retraction, a modified magnet-based force assay was used [31]. Magnetic beads were coated with crude pili preparations (CPPs) from piliated gonococci and added to T84 cells (Figure 4A). Within 30 min, small clusters of approximately two to ten beads attached to the cells, with each cell containing two to three clusters of beads (data not shown). Cell monolayers were then placed 10 mm beneath the magnet. At this distance, the magnet generates an upward force of 4 pN per bead (Figure 4B), or approximately 20–100 pN per cell.

T84 cells seeded with CPP-coated beads and exposed to the magnet were first examined for the presence of actin recruitment into cortical plaques (see Introduction). The clustering of actin near these beads would indicate that the magnetic force was sufficient to mimic pilus retraction forces from the bacterial microcolony. In the presence of magnetic

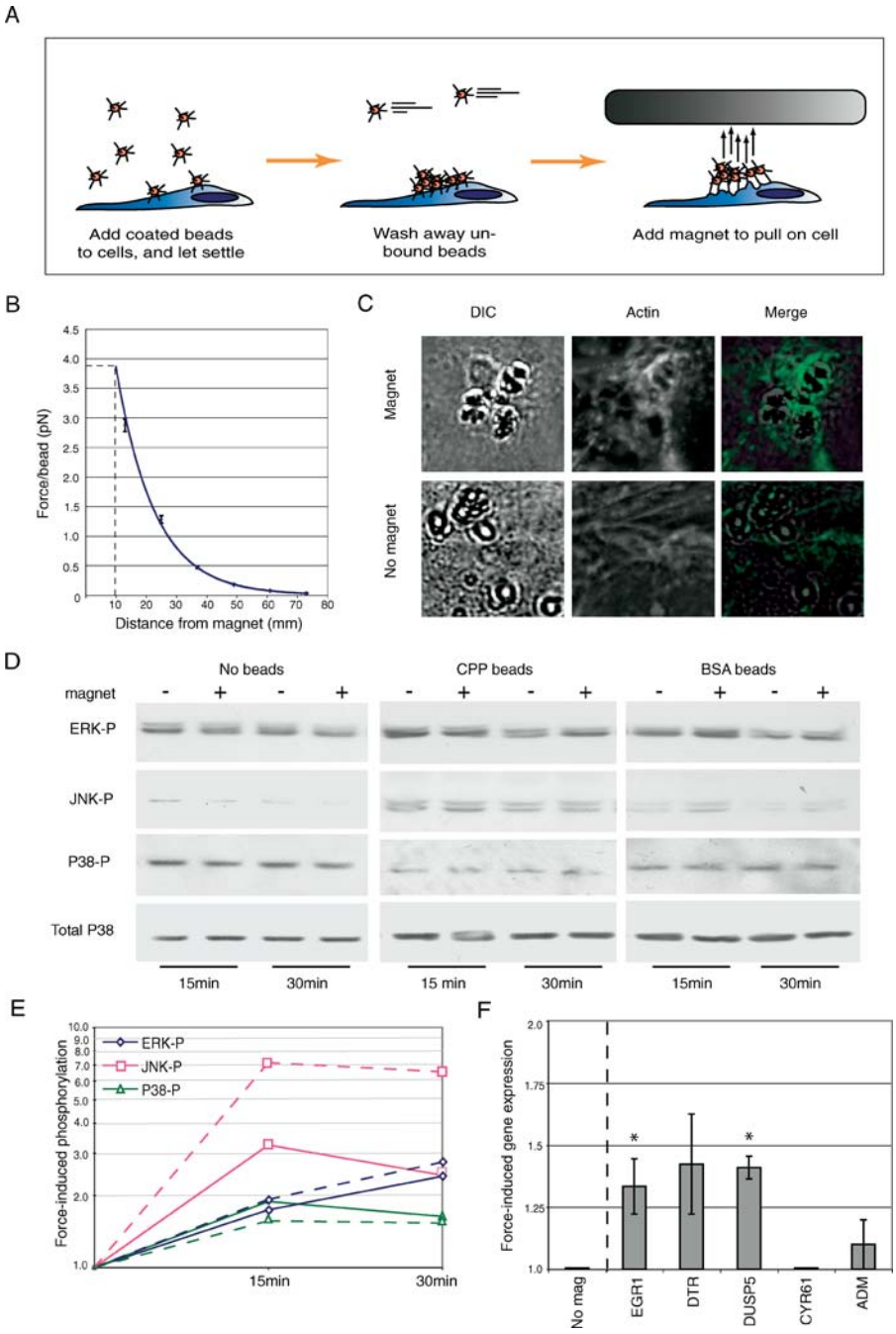

Figure 4. Artificial Force Triggers MAPK Phosphorylation and Induces the Expression of Retraction-Enhanced Genes

(A) Representation of the magnet/magnetic bead assay.

(B) Average force generated on one bead as a function of magnet distance from the culture dish. Data represent the forces calculated from four identical magnets (±SEM). All subsequent assays were performed using a magnet distance of 10 mm, which corresponds to a force of 4 pN per bead (dotted line).

(C) Magnet-induced clustering of actin beneath magnetic beads. CPP-coated beads were seeded onto T84 cells and exposed to the magnet for 1 h (top panels) or left untreated (no magnet, bottom panels). Differential interference contrast images (left panels) reveal the location of the beads; phalloidin staining (middle panels) shows the presence of actin at the same site. Right panels show the two previous images merged.

(D) Representative immunoblot of ERK-p, JNK-p, and P38-p in cells seeded with CPP-coated beads, BSA-coated beads, or no beads, and exposed to the magnet for 15 or 30 min. Total P38 protein levels in each sample served as the internal control (bottom panels).

(E) Quantitation of ERK-p, JNK-p, and P38-p signals by densitometry from the representative immunoblot shown in (D), normalized to the no-bead control. Solid lines indicate signals from cells exposed to membrane-coated beads; dotted lines indicate signals from cells exposed to BSA-coated beads.

(F) Real-time quantitative RT-PCR analysis of the transcript levels of selected genes in cells seeded with CPP beads and exposed to the magnet for 3 h. Data represent the average fold-change (±SEM, $n = 2$) compared to a no-magnet control. A significant difference in expression on force induction is denoted by an asterisk ($p < 0.1$).

DOI: 10.1371/journal.pbio.0030100.g004

force, actin concentrated in the cell cortex around membrane-coated beads (Figure 4C, top panel). In contrast, actin did not cluster with the beads in the absence of the magnet (Figure 4C, bottom panel). Thus, the force generated by this magnet system was sufficient to recruit actin to the site of the attached beads.

We next determined whether magnetic forces applied to CPP-coated beads were sufficient to activate MAPK and alter gene expression. The levels of all three phosphokinases were slightly reduced when the magnetic field was applied to cells incubated with medium alone (Figure 4D, no beads). Levels of each phosphorylated kinase from bead-treated samples (Figure 4D, CPP) were normalized to those from the no-bead samples to account for the effect of the magnet alone on MAPK phosphorylation. Following normalization, increased levels of all three phosphokinases are evident within the short time course (Figure 4E, solid lines).

In parallel experiments, cells were seeded with bovine serum albumin (BSA)-coated beads and exposed to the magnet. Under these conditions, less force was applied to the cells, as fewer bead clusters attached to the cells, and each cluster contained only two to three beads on average (data not shown). Again, levels of each phosphorylated kinase from bead-treated samples (Figure 4D, BSA beads) were normalized to those from the no-bead samples to account for the effect of the magnet alone on MAPK phosphorylation. Despite lower forces, BSA-coated beads also activated ERK, JNK, and P38 (Figure 4E, dashed lines). Interestingly, force-induced activation of both JNK and ERK was higher in cells treated with BSA-coated beads. This can most likely be attributed to the fact that BSA-coated beads, unlike CPP beads, induce no MAPK activation in the absence of force (data not shown). Thus when force-induced MAPK activation is calculated, the CPP-coated beads are normalized to a higher level of "background" activation than are the BSA-coated beads. The observation that force induction via both CPP- and BSA-coated beads can induce these signals strongly indicates that activation of MAPK cascades is, in part, a response to stress forces on the membrane rather than to force mediated through specific adhesin–receptor contacts between the bacterium and the host.

To examine the effect of mechanical stress on gene expression changes, cells seeded with CPP-coated beads were exposed to magnetic force for 3 h, and gene expression levels were analyzed by real-time quantitative RT-PCR. Transcript levels were expressed as the ratio of signals from magnet-stimulated cells to those from cells not subjected to magnetic force. All three "enhanced" genes tested, *EGR1, DTR,* and *DUSP5,* were upregulated in cells exposed to magnetic force (Figure 4F). In contrast, neither *ADM* (W/P $\approx$ 1.0) nor *cyr61* (which did not respond to MAPK inhibitors; see Figure 3E) was affected by the magnet.

In this and the previous experiment, magnet-induced changes were of lower magnitude than those induced by infection. The most plausible explanation for this difference is that pilus retraction from a microcolony likely generates greater force than a magnet acting on a small cluster of beads. In our magnet assay, an average force of 20–100 pN was placed on each cell. During an infection, each *pilus* can induce this amount of force. Thus, if there are 10–100 bacteria per microcolony, and each bacterium expressed 10 pili (a conservative estimate), pilus retraction from a single microcolony could place forces of 10^4–10^5 pN on the cell. Nonetheless, our method of artificial force application did indeed activate all three MAPK cascades and increased the expression level of each gene examined by approximately 1.5-fold. (Note that a minimum 1.5-fold change in expression level was found to accurately identify retraction-responsive genes in the microarray experiment.) Together, these results demonstrate that retraction-enhanced MAPK activation and gene expression changes can be replicated by artificial force.

Pilus Retraction Mediates Host Cell Cytoprotection

Many of the retraction-responsive genes are known to protect cells from apoptosis and from a variety of cellular stresses. Moreover, prolonged ERK activation accompanied by transient JNK and P38 activation (as observed in a wt infection; see Figure 3A and 3B) is hypothesized to mediate cytoprotection [32,33,34,35]. We therefore investigated whether pilus retraction was involved in determining cell fate by assaying infected cells for cleaved poly(ADP-ribose) polymerase (PARP) and cleaved caspase 8. PARP is a 116-kDa nuclear protein that mediates DNA repair in response to cell stress and is required to maintain cell viability [36,37]. During programmed cell death, the protein is cleaved by caspase 3 or caspase 7, a terminal step in the caspase cascade [38,39]. Caspase 8, however, is an initiator caspase that is upstream of caspase 3, caspase 7, and PARP, and represents an earlier event in the apoptosis cascade. Thus, increased levels of cleaved PARP or caspase 8 indicate that a cell is undergoing apoptosis.

Cells infected with N400 for 6 h contained lower levels of both cleaved PARP and cleaved caspase 8 than did uninfected cells (Figure 5A). In contrast, N400*pilT*-infected cells had higher levels of cleaved PARP and cleaved caspase 8 than did both uninfected and wt-infected cells. These results indicate that piliated gonococci that cannot retract pili induce low levels of programmed cell death in a culture. In contrast, gonococci capable of retracting their pili lower the tendency for cells to enter the apoptosis pathway.

We next determined whether this cytoprotective effect of pilus retraction was sufficient to protect cells from staurosporine (STS)-induced apoptosis. STS is a cell-permeant protein kinase inhibitor that induces apoptosis at micromolar concentrations [40,41]. Infection of urethral epithelium with *N. gonorrhoeae* was recently reported to protect these cells from STS-induced apoptosis [42]. Both N400 and N400*pilT* infection protected T84 cells from STS-induced apoptosis, as compared to uninfected cells (Figure 5B). However, cleaved PARP and cleaved caspase 8 levels in N400*pilT*-infected cells were higher than in wt-infected cells, indicating that pilus retraction enhances protection from STS-induced apoptosis.

Finally, we examined whether this retraction-enhanced cytoprotection is specifically mediated by mechanical force. In the absence of force, CPP-coated beads provided moderate protection from STS-induced apoptosis, demonstrated by lower cleaved PARP and cleaved caspase 8 levels than the no-bead cell control (Figure 5C). This result is similar to that seen in *pilT*-infected cells and suggests that components in the bacterial membrane are sufficient to protect against STS-induced apoptosis. Cells seeded with CPP-coated beads and exposed to the magnetic field had still lower cleaved PARP and cleaved caspase 8 levels, consistent with data from wt-

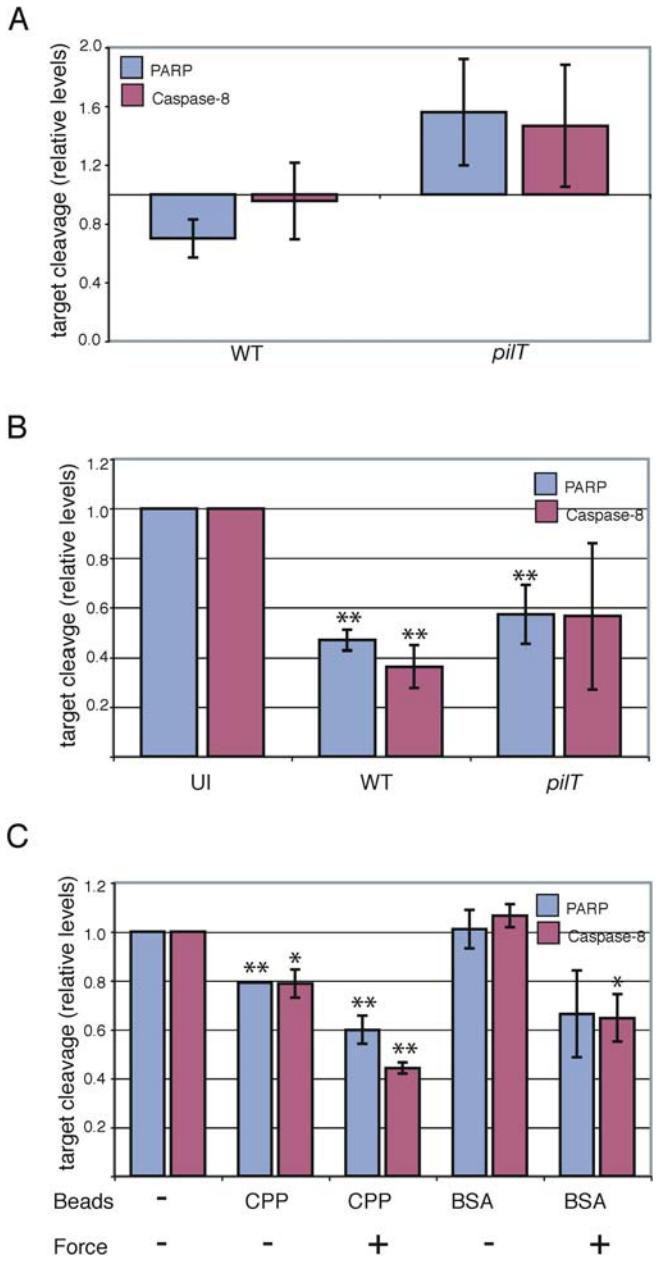

Figure 5. Pilus Retraction during Bacterial Attachment Promotes Host Cell Cytoprotection

(A) Levels of cleaved PARP and cleaved caspase 8 in T84 cells infected for 6 h with N400 (WT) or N400*pilT (pilT)*, normalized to cleaved PARP or cleaved caspase 8 levels in uninfected cells.

(B) Levels of cleaved PARP and cleaved caspase 8 in T84 cells infected with N400 (WT) or N400*pilT (pilT)* or left uninfected (UI) for 4 h, then incubated with STS (1 μM) for an additional 4 h to induce apoptosis. A significant difference from uninfected cells is denoted by two asterisks ($p < 0.05$).

(C) Cleaved PARP and cleaved caspase 8 levels in cells exposed to magnetic force. T84 cells were seeded with CPP- or BSA-coated beads and exposed to the magnet for 2 h or were left unexposed, then incubated with STS (1 μM) for an additional 4 h away from the magnet. The cleaved PARP and cleaved caspase 8 level in cells without beads and not exposed to magnetic force is arbitrarily assigned a value of 1.0, and all other treatments are expressed relative to this value. For all experiments, cleaved protein levels were quantified by densitometry of immunoblot signals. Values represent the mean levels of cleaved target (±SEM) from two independent experiments. A significant difference from untreated cells is denoted by two asterisks ($p < 0.05$) or by a single asterisk ($p < 0.1$).

DOI: 10.1371/journal.pbio.0030100.g005

infected cells (Figure 5B). BSA-coated beads did not protect against STS-induced apoptosis in the absence of magnetic force. However, when force was applied to these cells, the level of cleaved PARP and cleaved caspase 8 was reduced nearly to the value observed for membrane-coated beads in the presence of the magnet. Together, these data indicate that nonspecific membrane tension is capable of protecting the host cell against apoptosis.

Discussion

Retraction of the *N. gonorrhoeae* Tfp during bacterial attachment elicits host cell signaling cascades essential for the establishment of intimate attachment and promotion of bacterial invasion [17]. We tested the hypothesis that Tfp retraction induces changes in epithelial cell gene expression during bacterial attachment. Pilus retraction, per se, did not regulate a unique set of genes. Rather, retraction enhanced the expression of a small subset of infection-regulated genes (see Figure 1), many of which are known to respond specifically to mechanical stress and to be induced by the MAPK cascade. We confirmed that wt bacteria activated MAPKs ERK, JNK, and P38 at a higher level than the *pilT* mutant. Moreover, MAPK inhibitors lowered the expression level of all but one retraction-responsive gene selected for further examination (see Figure 3). These results strongly indicate that MAPK signaling plays a major role in the enhancement of gene expression by pilus retraction.

Importantly, artificial force placed on the cell membrane using magnets and magnetic beads can replicate the gene expression changes and MAPK activation observed using wt bacteria, indicating that pilus retraction may induce these events via mechanical force. Although the total force produced by pilus retraction within a bacterial microcolony is not known, we estimate that it is on the order of 10^4–10^5 pN, based on 100 pN per retraction event, approximately 10 pili per bacteria, and roughly 10–100 bacteria per microcolony. In comparison, this amount of force is equivalent to that applied to integrin complexes in the periodontal ligament by a human bite [31]. Retraction forces from a microcolony could therefore be physiologically relevant.

We cannot exclude the possibility that pilus retraction enhances these signaling events by mechanisms independent of membrane tension (i.e., through secondary receptor engagement or via an inherent difference in the pilus structure/composition between wt and *pilT* bacteria). Our data with CPP-coated beads strongly argue against these possibilities, however. The CPP preps used for bead coating were from wt cultures, and thus were identical. In addition, the magnet pulled the beads upward. This should pull the bead farther from the cell surface, making secondary receptor engagement less likely. The possibility remains, however, that pilus differences or secondary receptor engagement may act in concert with membrane tension to generate the higher levels of MAPK activation and gene expression changes seen with infection. Further research is needed to examine this possibility. Nonetheless, we are confident that force plays at least some role in the signaling events identified through this work.

We have begun to assess the biological functions of enhanced gene expression and MAPK activation during gonococcal infection. ERK, JNK, and P38 play a role in determining cell survival during stress and entry into the

apoptosis pathway [32]. Moreover, nearly half of the identified retraction-enhanced genes are known to be involved in cell cycle/survival signaling. We show that cells infected with wt bacteria have lower levels of cleaved PARP and cleaved caspase 8 than do uninfected and *pilT*-infected cells. Pilus retraction is therefore predicted to enhance the ability of the cell to withstand apoptosis-inducing signals generated by infection. Indeed, cells infected with wt bacteria withstood STS-induced apoptosis better than uninfected cells and cells infected with *pilT*.

The effect of *N. gonorrhoeae* infection on cell fate has been a long-standing controversy. The neisserial porin has been reported to protect cells from apoptosis [43] as well as to induce programmed cell death [44]. These conflicting observations are likely a result of differences in experimental systems and bacterial strains. We believe that our results may clarify the issue of *N. gonorrhoeae* and programmed cell death, through the identification of another bacterial factor (i.e., pilus retraction) involved in such a response.

A number of factors influence the ability of the cell to withstand apoptosis, including the signaling cascades that are activated and the degree and duration of the activation of these cascades [32]. They also include the virulence genes expressed by the infecting bacteria. The bacterial strains used for previous studies on *N. gonorrhoeae* and apoptosis differed in their piliation state and their ability to invade the host cell. Our results indicate that piliated bacteria, in the absence of pilus retraction, slightly increase the tendency of the infected cell to undergo apoptosis (see Figure 5A). However, these bacteria are still able to moderately protect infected cells from STS-induced apoptosis, indicating that a certain level of cytoprotection is provided by other bacterial factors. In contrast, bacteria that can retract their pili, and thus presumably induce mechanical stress on the host-cell membrane, strongly mediate pro-survival signaling.

The influence of mechanical stress on apoptosis has been studied in some detail. Importantly, such studies indicate that different stress patterns result in different cellular outcomes. Extended, repetitive mechanical force increases the expression of genes encoding cytoprotective heat shock proteins and lowers the number of apoptotic cells in a culture [45]. Suppression of apoptosis requires permanent membrane tension or rhythmic, pulsatile forces [46], which are thought to allow the cell to adapt to new environmental conditions. Retraction events in *N. gonorrhoeae* generate strong, pulsatile forces every 1–20 s [13]. The nature of the pilus retraction force may therefore be the key to counteracting infection-induced apoptosis. Our data strongly indicate that pilus retraction from a microcolony is capable of stimulating mechanoprotective signals.

In light of the results presented here and elsewhere, we propose a model to explain how pilus retraction by *N. gonorrhoeae* influences survival signaling in the infected cell (Figure 6). Initial contact between the bacterium and the epithelial cell activates MAP kinases and alters gene expression at a low level. The cell senses "stress" from the infection, the degree of which varies depending on the metabolic state of the cell and the constellation of virulence factors expressed by the infecting strain. As a result of this stress, the cell is poised to enter the apoptosis pathway. In the absence of pilus retraction and membrane tension, the low levels of activated MAP kinases may or may not be enough to counteract this stress. As the infection proceeds, microcolonies are formed. Pilus retraction from microcolonies is hypothesized to exert stress forces on the membrane, amplifying the levels of activated MAPK, enhancing the transcription of infection-induced genes, and possibly activating other as-yet-unidentified pathways. The end result is the enhanced stimulation of pro-survival pathways and an overriding of pro-apoptotic stress signals. In other words, the fate of the infected cell is decided by the type of signaling networks induced by infection and the extent of activation of these networks. Pilus retraction tips the balance in favor of cell survival.

We have used a tissue culture system to study the interplay between pilus retraction, host cell signaling, and gene expression during the attachment phase of *N. gonorrhoeae* infection. How these interactions may affect the disease in vivo remains to be clarified. Our results make teleologic sense when the bacterial life cycle and gonococcal disease are taken into consideration. *N. gonorrhoeae* does not survive on fomites and has no intermediate host. Transmission depends on person-to-person spread. Simple mucosal gonorrhea infections can be mild, and inflammatory responses begin days after exposure [47]. Moreover, a significant number of infected individuals carry gonococci without overt symptoms of disease [47,48]. Indeed, the ability of the bacterium to survive as a species requires a relatively healthy host. Our model for pilus retraction is consistent with these considerations.

Materials and Methods

Reagents. Antibodies to PARP, caspase 8, c-Jun, phospho-c-Jun

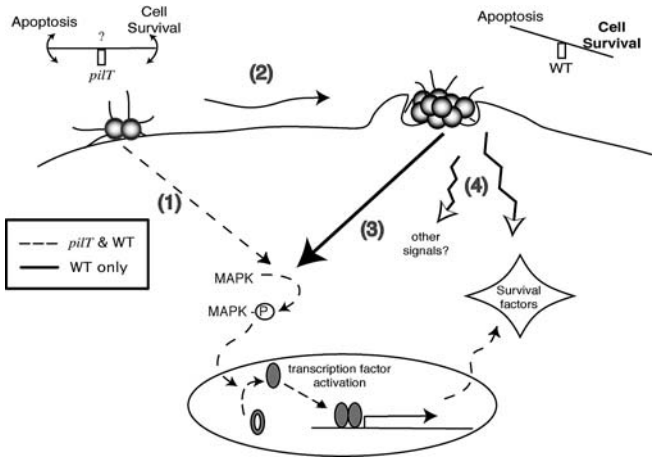

Figure 6. Model of the Role of Pilus Retraction in Promoting a Cytoprotective Environment during Gonococcal Infection of an Epithelial Cell

(1) Initial contact between the bacterium and host cell activates low levels of MAPK, and transcription of infection-induced genes. This level of signaling may or may not be able to protect the cell from apoptosis; thus, the host cell "teeters" on the edge of life and death.
(2) As the infection proceeds, microcolonies of gonococci are formed, and more pili are locally available to retract.
(3) Pilus retraction amplifies MAPK activation, which in turn enhances the transcription of mechanical stress–induced genes.
(4) Pilus retraction may also stimulate other pathways that mediate gene expression and survival signaling. Overall signaling events tip the balance in favor of cell survival.
DOI: 10.1371/journal.pbio.0030100.g006

(Ser63), P44/42 MAPK, phospho-p44/42 MAPK (Thr202/Tyr204), phospho-MAPKAPK2 (Thr334), p38 MAPK, phospho-p38 MAPK (Thr108/Tyr182), SAPK/JNK, and phospho-SAPK/JNK (Thr183/Tyr185) were purchased from Cell Signaling Technology (Beverly, Massachusetts, United States). MAPK inhibitors SB203588, U0126, and SP600125 were purchased from Calbiochem (San Diego, California, United States) and used at a final concentration of 10 μM unless otherwise stated. STS was purchased from Cell Signaling Technology and used at a final concentration of 1 μM to induce apoptosis. Neodymium iron boron (NdFeB) magnets (Eneflux Armtek Magnetics, Bethpage, New York, United States) measured 2 in. in diameter by 1 in. thick and were grade 30 (MGOe).

Cell lines, bacterial strains, and infections. T84 human colonic epidermoid cells (American Type Culture Collection, Manassas, Virginia, United States) were maintained in DMEM-F-12 plus 5% heat-inactivated, filter-sterilized fetal bovine serum at 37 °C and 5% CO_2. For all experiments, cells were seeded into 35-mm dishes and allowed to become confluent before infection. *N. gonorrhoeae* strains N400 and N400*pilT* [49] were used for all infections and were maintained on GCB agar plus Kellogg's supplements at 37 °C and 5% CO_2. Piliation and Opa phenotypes were monitored by colony morphology. Only piliated, Opa^- bacteria were used. For infection experiments, bacteria were resuspended in GCB liquid medium and added to the epithelial cells at a multiplicity of infection of 50.

RNA isolation and microarray analysis. T84 cells were infected with N400 or N400*pilT* or treated with GCB medium alone for 3 h. For RNA isolation, labeling, and microarray hybridization procedures, see Protocol S1. Comparative analysis was performed using MAS 5.0 algorithms to determine fold-change values between uninfected and infected samples from the same experiment, with uninfected samples representing the baseline. Statistical analysis was performed on natural-log transformed data using Cyber-T (http://visitor.ics.uci.edu/genex/cybert/). Subsequent data analysis was performed using Excel (Microsoft, Redmond, Washington, United States) and GeneSpring version 4.0 (Silicon Genetics, Redwood City, California, United States). Genes with a "presence call" *p*-value of less then 0.1 across all chips were eliminated from analysis, as were genes that were given a "no change" call across all samples. A gene was identified as differentially regulated if the fold-change was greater than ±1.5 in at least two out of three experiments. "Enhanced" genes were identified by calculating the ratio of the fold-change for the wt-infected cells to the fold-change for the *pilT*-infected cells (W/P). Gene expression was considered to be enhanced by pilus retraction if the W/P, averaged from at least two out of three individual experiments, was greater than 1.5, and the individual W/P from each experiment was greater than1.25.

Real-time RT-PCR analysis. One microgram of total RNA (as isolated above) was reverse-transcribed to generate cDNA, using the iScript cDNA synthesis kit (Bio-Rad, Hercules, California, United States). As a control, parallel samples were run in which reverse transcriptase was omitted from the reaction mixture. Quantitative real-time PCR was performed using an ABI PRISM 7000 Sequence Detection System (Applied Biosystems, Foster City, California, United States). Amplification was carried out using TaqMan master mix (Applied Biosystems), and pre-designed TaqMan probes (Assays on Demand, Applied Biosystems) according to the manufacturer's instructions. Assay numbers are given in Table 1. Reactions were performed in triplicate in a 20-μl volume, with the following cycle parameters: 95 °C/10 min enzyme activation, 95 °C/15 s, 60 °C/1 min for 40 cycles. Data analysis was performed using the comparative Ct method (Applied Biosystems) to determine relative expression levels.

Immunoblotting. T84 cells were infected with N400 or N400*pilT* or treated with GCB medium alone for specified times. Following infection, cells were lysed with 150 μl of 1× SDS lysis buffer (62.5 mM Tris-HCl [pH 6.8], 2% w/v SDS, 10% glycerol, 50 mM DTT, 0.1% w/v bromophenol blue), scraped into Eppendorf tubes, vortexed for 15 s, and immediately stored at −20 °C. For PARP and caspase 8 assays, samples were incubated with 150 μl of cell lysis buffer (20 mM Tris [pH 7.5], 150 mM NaCl, 1 mM EDTA, 1 mM EGTA, 1% Triton X-100, 0.5% NP40, 2.5 mM sodium pyrophosphate, 1 mM β-glycerolphosphate, 1 mM Na_3VO_4, 1 μg/ml Leupeptin) for 20 min on ice, followed by a 15-s sonication. Samples were boiled for 5 min at 100 °C, then separated by SDS 8% polyacrylamide gels and transferred onto nitrocellulose sheets. Membranes were probed with the specified antibodies following the manufacturer's protocol.

CPPs and bead coating. *N. gonorrhoeae* CPPs were generated from piliated, Opa^- gonococci. Bacteria were scraped from overnight cultures (grown on plates) into HBSS and vortexed for 2 min, followed by centrifugation at 14,000*g* for 5 min. Supernatants were removed, quantitated by spectrophotometric analysis, and stored at −80 °C until use. Pili preparations were assayed for the presence of pili via indirect immunofluorescence microscopy and immunoblot, using anti-pilin antibody (data not shown). Bio-Mag Plus carboxy-modified paramagnetic microspheres (Bangs Laboratories, Fishers, Indiana, United States), were activated with 1-ethyl-3-(3-dimethylaminopropyl) carbodiimide, hydrochloride (EDAC), and incubated with piliated *N. gonorrhoeae* CPPs or BSA as per the manufacturer's instructions. Bead coating was confirmed by immunoblotting using antibodies to BSA (ICN Biomedicals, Irvine, California, United States) and pilin (antibody SM1; data not shown).

Table 1. Assays on Demand (TaqMan Probes and Primers) Used for Real-Time Quantitative RT-PCR in This Study

Gene	RefSeq ID	Assay Number	Description
GAPDH	NM_002046	Hs99999905_m1	Glyceraldehyde-3-phosphate dehydrogenase
EGR1	NM_001964	Hs00152928_m1	Early-growth response 1
DUSP2	NM_004418	Hs00358879_m1	Dual-specificity phosphatase 2
DUSP5	NM_004419	Hs00244839_m1	Dual-specificity phosphatase 5
IL-6	NM_000600	Hs00174131_m1	Interleukin 6
GADD45B	NM_015675	Hs00169587_m1	Growth arrest and DNA-damage-inducible, beta
TNFa	NM_000594	Hs00174128_m1	Tumor necrosis factor
CYR61	NM_001554	Hs00155479_m1	Cysteine-rich, angiogenic inducer, 61
Fos	NM_005252	Hs00170630_m1	C-fos
DTR	NM_001945	Hs00181813_m1	Diphtheria toxin receptor
NR4A1	NM_173158	Hs00544986_m1	Nuclear receptor subfamily 4, group A, member 1
Jun	NM_002228	Hs00277190_s1	C-Jun
ADM	NM_001124	Hs00181605_m1	Adrenomedullin
DUSP6	NM_001946	Hs00169257_m1	Dual-specificity phosphatase 6
DUSP10	NM_144728	Hs00200527_m1	Dual-specificity phosphatase 10
KIF13B	NM_015254	Hs00209573_m1	Kinesin family member 13B
AKAP12	NM_005100	Hs00374507_m1	A kinase (PRKA) anchor protein (gravin) 12
TBCC	NM_003192	Hs00268437_s1	Tubulin-specific chaperone c

DOI: 10.1371/journal.pbio.0030100.t001

Immunofluorescence microscopy. T84 cells were grown on coverslips to 50% confluency and incubated with either BSA-coated or CMP-coated magnetic beads for 15 min. Unbound beads were washed off and the magnet placed at a distance of 10 mm from the cell surface for 1 h. The medium was then aspirated, and the cells fixed for 15 min at room temperature in 4% paraformaldehyde. Cells were blocked and permeabilized in isotonic PBS containing BSA (3%, w/v) and saponin (0.02% w/v) for 1 h at room temperature, followed by staining with Alexa-Fluor 594 phalloidin (Molecular Probes, Eugene, Oregon, United States) at 1:1,000 for 30 min. Samples were rinsed extensively in PBS before mounting in Fluoromount-G (Fisher Scientific, Hampton, New Hampshire, United States). Images were obtained with a Deltavision Restoration Microscope (Applied Precision, Issaquah, Washington, United States) fitted with a Nikon (Tokyo, Japan) 60× oil-immersion objective and processed at a Silicon Graphics (Mountain View, California, United States) workstation with accompanying API software. The images were subsequently exported to Adobe Photoshop (version 7.0) and Adobe Illustrator (version 11.0) (Adobe Systems, San Jose, California, United States) for manuscript preparation.

Calculation of magnetic force. To quantify the amount of force that the magnet exerts per magnetic bead, the change-in-mass method [31] was used. Briefly, the mass of a known number of dry beads (0.12 g) was measured on an electronic balance in the presence and absence of the magnet. Given the mean bead diameter of 1.5 μm and the bead density of 2.5×10^3 kg/m^3 (Bangs Laboratories), the number of beads in this sample was calculated to be 1.2×10^{10}. The change in mass of the beads in the presence of the magnet was entered into the equation—force = Δmass × acceleration (with acceleration being equal to gravity, or 9.81 m/s^2)—to give a value for the force. Change-in-mass measurements were taken at varying distances from the magnet to determine force as a function of distance (see Figure 4B).

Magnetic force experiments. T84 cells were grown to confluency in 35-mm culture dishes. Before assay, the cells were incubated with prewarmed, serum-free medium for 2 h. Cells were then incubated

for 30 min with medium alone, or with CPP- or BSA-coated beads diluted in the same medium. Cells were then washed with fresh, serum-free medium to remove unbound beads. Magnets were placed at a distance of 10 mm from the bottom of the tissue culture dish, and the dishes were incubated for the specified time at 37 °C, 5% CO_2. The samples were then processed for RNA isolation or SDS-PAGE, as described above. Control samples were treated in parallel but were not exposed to the magnet.

Statistics. Statistical analysis was performed using standard *t*-test analysis with SPSS version 11.0 (SPSS, Chicago, Illinois, United States) unless otherwise stated.

Supporting Information

Protocol S1. MIAME Checklist

Found at DOI: 10.1371/journal.pbio.0030100.sd001 (42 KB DOC).

Table S1. Supplementary References

Found at DOI: 10.1371/journal.pbio.0030100.st001 (409 KB DOC).

Accession Numbers

The GenBank (http://www.ncbi.nlm.nih.gov/Genbank/) accession numbers for the genes and gene products discussed in this paper are *ADM* (D14874), *cyr61* (Y11307), DTR (M60278), *DUSP5* (U15932), EGR1 (X52541), PilF (U32588), and PilT (S72391).

Acknowledgments

We wish to thank S. W. Lee, J. Larson, and A. Friedrich for their thoughtful suggestions and careful reading of the manuscript. We also wish to thank the Affymetrix Microarray Core (OHSU Gene Microarray Shared Resource) for performing RNA labeling and hybridization. This work was supported in part by National Institutes of Health grant RO1-AI049973 awarded to MS, and National Institutes of Health grant T32-AI07472 awarded to HLH.

Competing interests. The authors have declared that no competing interests exist.

Author contributions. HLH and MS conceived and designed the experiments. HLH performed the experiments and analyzed the data. MG and MS contributed reagents/materials/analysis tools. HLH and MS wrote the paper. ∎

References

1. Mattick JS (2002) Type IV pili and twitching motility. Annu Rev Microbiol 56: 289–314.
2. Wall D, Kaiser D (1999) Type IV pili and cell motility. Mol Microbiol 32: 1–10.
3. O'Toole GA, Kolter R (1998) Flagellar and twitching motility are necessary for *Pseudomonas aeruginosa* biofilm development. Mol Microbiol 30: 295–304.
4. Bechet M, Blondeau R (2003) Factors associated with the adherence and biofilm formation by *Aeromonas caviae* on glass surfaces. J Appl Microbiol 94: 1072–1078.
5. Dubnau D (1999) DNA uptake in bacteria. Annu Rev Microbiol 53: 217–244.
6. Yoshida T, Kim SR, Komano T (1999) Twelve pil genes are required for biogenesis of the R64 thin pilus. J Bacteriol 181: 2038–2043.
7. Karaolis DK, Somara S, Maneval DR Jr, Johnson JA, Kaper JB (1999) A bacteriophage encoding a pathogenicity island, a type-IV pilus and a phage receptor in cholera bacteria. Nature 399: 375–379.
8. Bieber D, Ramer SW, Wu CY, Murray WJ, Tobe T, et al. (1998) Type IV pili, transient bacterial aggregates, and virulence of enteropathogenic *Escherichia coli*. Science 280: 2114–2118.
9. Comolli JC, Hauser AR, Waite L, Whitchurch CB, Mattick JS, et al. (1999) *Pseudomonas aeruginosa* gene products PilT and PilU are required for cytotoxicity in vitro and virulence in a mouse model of acute pneumonia. Infect Immun 67: 3625–3630.
10. Merz AJ, Enns CA, So M (1999) Type IV pili of pathogenic *Neisseriae* elicit cortical plaque formation in epithelial cells. Mol Microbiol 32: 1316–1332.
11. Zolfaghar I, Evans DJ, Fleiszig SM (2003) Twitching motility contributes to the role of pili in corneal infection caused by *Pseudomonas aeruginosa*. Infect Immun 71: 5389–5393.
12. Pujol C, Eugene E, Marceau M, Nassif X (1999) The meningococcal PilT protein is required for induction of intimate attachment to epithelial cells following pilus-mediated adhesion. Proc Natl Acad Sci U S A 96: 4017–4022.
13. Merz AJ, So M, Sheetz MP (2000) Pilus retraction powers bacterial twitching motility. Nature 407: 98–102.
14. Henrichsen J (1983) Twitching motility. Annu Rev Microbiol 37: 81–93.
15. Freitag NE, Seifert HS, Koomey M (1995) Characterization of the pilF-pilD pilus-assembly locus of *Neisseria gonorrhoeae*. Mol Microbiol 16: 575–586.
16. Whitchurch CB, Hobbs M, Livingston SP, Krishnapillai V, Mattick JS (1991) Characterisation of a *Pseudomonas aeruginosa* twitching motility gene and evidence for a specialised protein export system widespread in eubacteria. Gene 101: 33–44.
17. Merz AJ, So M (2000) Interactions of pathogenic neisseriae with epithelial cell membranes. Annu Rev Cell Dev Biol 16: 423–457.
18. Maier B, Potter L, So M, Long CD, Seifert HS, et al. (2002) Single pilus motor forces exceed 100 pN. Proc Natl Acad Sci U S A 99: 16012–16017.
19. Shao JY, Ting-Beall HP, Hochmuth RM (1998) Static and dynamic lengths of neutrophil microvilli. Proc Natl Acad Sci U S A 95: 6797–6802.
20. Raucher D, Sheetz MP (2000) Cell spreading and lamellipodial extension rate is regulated by membrane tension. J Cell Biol 148: 127–136.
21. Choquet D, Felsenfeld DP, Sheetz MP (1997) Extracellular matrix rigidity causes strengthening of integrin-cytoskeleton linkages. Cell 88: 39–48.
22. Sheetz MP, Felsenfeld DP, Galbraith CG (1998) Cell migration: Regulation of force on extracellular-matrix-integrin complexes. Trends Cell Biol 8: 51–54.
23. Glogauer M, Ferrier J, McCulloch CA (1995) Magnetic fields applied to collagen-coated ferric oxide beads induce stretch-activated Ca2+ flux in fibroblasts. Am J Physiol 269: C1093–C1104.
24. Wu Z, Wong K, Glogauer M, Ellen RP, McCulloch CA (1999) Regulation of stretch-activated intracellular calcium transients by actin filaments. Biochem Biophys Res Commun 261: 419–425.
25. Wasserman SM, Mehraban F, Komuves LG, Yang RB, Tomlinson JE, et al. (2002) Gene expression profile of human endothelial cells exposed to sustained fluid shear stress. Physiol Genomics 12: 13–23.
26. McCormick SM, Frye SR, Eskin SG, Teng CL, Lu CM, et al. (2003) Microarray analysis of shear stressed endothelial cells. Biorheology 40: 5–11.
27. Ohki R, Yamamoto K, Mano H, Lee RT, Ikeda U, et al. (2002) Identification of mechanically induced genes in human monocytic cells by DNA microarrays. J Hypertens 20: 685–691.
28. Feng Y, Yang JH, Huang H, Kennedy SP, Turi TG, et al. (1999) Transcriptional profile of mechanically induced genes in human vascular smooth muscle cells. Circ Res 85: 1118–1123.
29. Naumann M, Rudel T, Wieland B, Bartsch C, Meyer TF (1998) Coordinate activation of activator protein 1 and inflammatory cytokines in response to *Neisseria gonorrhoeae* epithelial cell contact involves stress response kinases. J Exp Med 188: 1277–1286.
30. Hauck CR, Meyer TF, Lang F, Gulbins E (1998) CD66-mediated phagocytosis of Opa52 *Neisseria gonorrhoeae* requires a Src-like tyrosine kinase- and Rac1-dependent signalling pathway. EMBO J 17: 443–454.
31. Glogauer M, Ferrier J (1998) A new method for application of force to cells via ferric oxide beads. Pflugers Arch 435: 320–327.
32. Wada T, Penninger JM (2004) Mitogen-activated protein kinases in apoptosis regulation. Oncogene 23: 2838–2849.
33. Lin A (2003) Activation of the JNK signaling pathway: Breaking the brake on apoptosis. Bioessays 25: 17–24.
34. Davis RJ (2000) Signal transduction by the JNK group of MAP kinases. Cell 103: 239–252.
35. Roulston A, Reinhard C, Amiri P, Williams LT (1998) Early activation of c-Jun N-terminal kinase and p38 kinase regulate cell survival in response to tumor necrosis factor alpha. J Biol Chem 273: 10232–10239.
36. Satoh MS, Lindahl T (1992) Role of poly(ADP-ribose) formation in DNA repair. Nature 356: 356–358.
37. Oliver FJ, de la Rubia G, Rolli V, Ruiz-Ruiz MC, de Murcia G, et al. (1998) Importance of poly(ADP-ribose) polymerase and its cleavage in apoptosis. Lesson from an uncleavable mutant. J Biol Chem 273: 33533–33539.
38. Nicholson DW, Ali A, Thornberry NA, Vaillancourt JP, Ding CK, et al. (1995) Identification and inhibition of the ICE/CED-3 protease necessary for mammalian apoptosis. Nature 376: 37–43.
39. Tewari M, Quan LT, O'Rourke K, Desnoyers S, Zeng Z, et al. (1995) Yama/CPP32 beta, a mammalian homolog of CED-3, is a CrmA-inhibitable protease that cleaves the death substrate poly(ADP-ribose) polymerase. Cell 81: 801–809.
40. Couldwell WT, Hinton DR, He S, Chen TC, Sebat I, et al. (1994) Protein kinase C inhibitors induce apoptosis in human malignant glioma cell lines. FEBS Lett 345: 43–46.
41. Yue TL, Wang C, Romanic AM, Kikly K, Keller P, et al. (1998) Staurosporine-induced apoptosis in cardiomyocytes: A potential role of caspase-3. J Mol Cell Cardiol 30: 495–507.
42. Binnicker MJ, Williams RD, Apicella MA (2003) Infection of human urethral epithelium with *Neisseria gonorrhoeae* elicits an upregulation of host anti-apoptotic factors and protects cells from staurosporine-induced apoptosis. Cell Microbiol 5: 549–560.
43. Massari P, King CA, Ho AY, Wetzler LM (2003) Neisserial PorB is translocated to the mitochondria of HeLa cells infected with *Neisseria meningitidis* and protects cells from apoptosis. Cell Microbiol 5: 99–109.
44. Muller A, Gunther D, Dux F, Naumann M, Meyer TF, et al. (1999) Neisserial porin (PorB) causes rapid calcium influx in target cells and

induces apoptosis by the activation of cysteine proteases. EMBO J 18: 339–352.
45. Barkhausen T, van Griensven M, Zeichen J, Bosch U (2003) Modulation of cell functions of human tendon fibroblasts by different repetitive cyclic mechanical stress patterns. Exp Toxicol Pathol 55: 153–158.
46. Graf R, Apenberg S, Freyberg M, Friedl P (2003) A common mechanism for the mechanosensitive regulation of apoptosis in different cell types and for different mechanical stimuli. Apoptosis 8: 531–538.
47. Morse S (1996) *Neisseria, Branhamella, Moraxella,* and *Acinetobacter*. In: Baron S, editor. Medical microbiology, 4th ed. Galveston (Texas): University of Texas Medical Branch.
48. Turner CF, Rogers SM, Miller HG, Miller WC, Gribble JN, et al. (2002) Untreated gonococcal and chlamydial infection in a probability sample of adults. JAMA 287: 726–733.
49. Wolfgang M, Park HS, Hayes SF, van Putten JP, Koomey M (1998) Suppression of an absolute defect in type IV pilus biogenesis by loss-of-function mutations in pilT, a twitching motility gene in *Neisseria gonorrhoeae*. Proc Natl Acad Sci U S A 95: 14973–14978.